PHYSICAL REVIEW B VOLUME 47, NUMBER 15 15 APRIL 1993-I

Effect of reservoir-electron motion on the frequency response of double-barrier resonant tunneling

Akira Sugimura*
NTT Basic Research Laboratories, Musashino-shi, Tokyo 180, Japan
(Received 31 March 1992; revised manuscript received 16 November 1992)

The frequency response of the double-barrier resonant-tunneling current to the bias-voltage modulation is studied theoretically taking into account the effect of the dynamic motion of reservoir electrons in the contacts. A density-matrix approach with a transfer Hamiltonian is used and the incoherent scatterings in the contacts are modeled with damping constants. It is shown that the bandwidth of the device is determined not only by the electron-transfer rates through the barriers but also by the phase-smearing rates for the tunneling electrons. It is also shown that the frequency response of the tunneling current exhibits resonance enhancements in the high-frequency region. The enhancements are attributed to the quantum oscillations of the electrons between the quantum well and contact regions.

I. INTRODUCTION

The double-barrier resonant-tunneling structure has been extensively studied since its proposal by Tsu, Esaki, and Chang.[1,2] The interest in this system was increased by experiments[3] showing a high-speed frequency response up to several THz. Although there are many important aspects to be clarified in this device, such as phonon-assisted tunneling,[4–6] the effect of electron-electron interaction,[7] and noise characteristics,[8] the dynamic properties of the device would have to be considered one of the most important.

The frequency response has been discussed theoretically using various formalisms such as Wigner function formulas[9–11] and nonequilibrium Green functions.[12,13] These enable us to treat the resonant tunneling as a quantum transport phenomenon based on quantum statistical mechanics. According to these results, linear frequency response is basically a decreasing function with respect to the modulation frequency ω, when ω is higher than the inverse of the characteristic tunneling time through a barrier. Therefore, when the barriers are thick, the device will not respond to a very high-frequency modulation. On the other hand, the calculation in Ref. 11 shows a resonance peak for the nonlinear frequency response, which, the author suggested, is responsible for the experimental data reported in Ref. 3.

The double-barrier tunneling-device structure can be separated into three parts: a ballistic region and two contact regions which are subjected to the reservoirs. Because we may assume, in the ideal device, that the motion of the electrons in the ballistic region is not directly affected by any scatterings, electron waves in the ballistic region are considered to be coherently continuous. In the contacts, the electron wave will suffer from the scatterings by other electrons or phonons, so that it is no longer completely coherent. However, since the scattering process is stochastic, the electron wave must be partially coherent to show the wave nature near the boundary in the contact region. The importance of the scattering effect in this region was pointed out in Refs. 14 and 15, where the static behavior of the tunneling was studied. This effect will be much more important when we discuss the dynamic motion of the resonant tunneling.

In the present paper, we discuss the dynamic property of double-barrier resonant tunneling. We use a transfer-Hamiltonian, density-matrix approach and a boundary condition that does not reject the effects of the wave nature in the electrodes.[14] We use this approach to discuss the small-signal frequency response. It will be shown that the linear response exhibits resonance enhancements in the high-frequency region due to the quantum oscillations of the electrons between the quantum-well and contact regions.

II. RESPONSE FREQUENCY UNDER SMALL-SIGNAL MODULATION

The schematic potential profile of the resonant-tunneling structure is shown in Fig. 1. The electronic densities at the contacts I and III are assumed to be high enough to maintain the flat potential, so that the voltage drop across the device is concentrated at the double barriers.

The starting equations for the present analysis are the same as those in Ref. 14, where the density-matrix approach was used. We use the electron wave functions localized in each region I, II, and III, as basis functions to expand the tunneling system. The annihilation and creation operators are defined as a_{ij} and $a_{ij}^{\dagger}$ for the quantum state j in the region i, where $i=1$, 2, and 3, respectively, correspond to the left contact, the quantum well, and the right contact. The transfer Hamiltonian used to describe the coherent interaction is

$$H_{\mathrm{coh}}=-\sum_{j,k}[t_L a_{1j}^{\dagger}a_{2k}+\mathrm{H.c.}]-\sum_{k,m}[t_R a_{2k}^{\dagger}a_{3m}+\mathrm{H.c.}]+\sum_{j}\varepsilon_{1j}a_{1j}^{\dagger}a_{1j}+\sum_{k}\varepsilon_{2k}a_{2k}^{\dagger}a_{2k}+\sum_{m}\varepsilon_{3m}a_{3m}^{\dagger}a_{3m}\ . \quad (1)$$

Here ε_{ij} is the total energy of the one-electron state a_{ij}, and H.c. indicates the Hermitian conjugate. The transfer energies t_L and t_R through the left and right barriers are

 ©1993 The American Physical Society

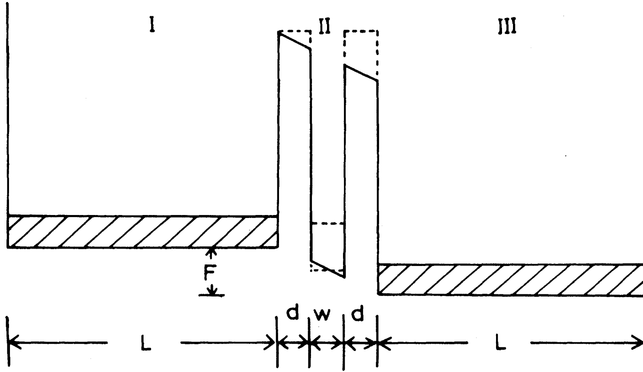

FIG. 1. The schematic potential profile for a double-barrier resonant-tunneling structure. Regions I and III are contact regions that extend a distance of L. Region II is a quantum well with a well width of w and a barrier width of d. A dc bias voltage F with a small-signal modulation is externally applied to this structure.

defined by the overlap integrals of basis wave functions, as given in Ref. 14.

Each contact region is considered to be locally in thermal equilibrium with a differently fixed chemical potential, because only a small part of the electrons in the contact are involved in the tunneling process. The thermalization is achieved by the electron-electron or electron-phonon interactions inside each contact. This is expressed by the interaction Hamiltonian H_1 or H_3, which includes only the variables of each contact and is independent of the position operators. These Hamiltonians cause the fluctuation and dissipation for the system operators.[16] This dissipation gives rise to the damping of the density operator matrix elements to their local equilibrium values with corresponding damping constants.[17] Thus the electrons in each contact, as a reservoir, cause the incoherent damping of the density operator $\rho_{i,j}$ to its equilibrium state with the damping constant $\gamma_{i,j}$. Here i and j range from 1 to 3, corresponding to the regions I–III. Although the quantitative dependence of the damping constants on quantum states can be obtained[17] by using the second-order perturbation theory and integrating out the reservoir variables, here we treat them as constant parameters.

The total motion of $\rho_{i,j}$ is thus given by adding the incoherent damping motion caused by the reservoir to the coherent motion caused by H_{coh} as expressed by

$$\frac{d\rho_{ij}}{dt}=\frac{i}{\hbar}[H_{\text{coh}},\rho]_{i,j}+\gamma_{i,j}(f_i\delta_{i,j}-\rho_{i,j}) , \tag{2}$$

where f_i are quasi-Fermi-distribution functions of the electrons in each region and $\delta_{i,j}$ is the Kronecker delta.

We now specify the system with only one quantum sublevel, which has energy ε_2, in II. We assume that there are no scattering processes for electrons in II, which is equivalent to the condition that γ_{22} is zero. Then electron momenta k_x and k_y, in the x-y plane perpendicular to the tunneling direction, are conserved. We can then integrate Eq. (2) with respect to x and y coordinates, resulting in

$$\begin{aligned}\frac{dN_1}{dt}=&-\frac{it_L}{\hbar}D_1(\varepsilon_{1l'})J_{12}+\frac{it_L}{\hbar}D_1(\varepsilon_{1l})J_{21}\\&-\frac{i}{\hbar}(\varepsilon_{1l}-\varepsilon_{1l'})N_1\\&+\gamma_{11}[D_1(\varepsilon_{1l'})F_1(\varepsilon_{1l})\delta_{\varepsilon_{1l},\varepsilon_{1l'}}-N_1] ,\end{aligned} \tag{3}$$

$$\frac{dN_2}{dt}=-\sum_{\varepsilon_{3l}}\frac{it_R}{\hbar}[J_{23}-J_{32}]+\sum_{\varepsilon_{1l}}\frac{it_L}{\hbar}[J_{12}-J_{21}] , \tag{4}$$

$$\begin{aligned}\frac{dN_3}{dt}=&\frac{it_R}{\hbar}D_3(\varepsilon_{3l})J_{23}-\frac{it_R}{\hbar}D_3(\varepsilon_{3l'})J_{32}-\frac{i}{\hbar}(\varepsilon_{3l}-\varepsilon_{3l'})N_3\\&+\gamma_{33}[D_3(\varepsilon_{3l'})F_3(\varepsilon_{3l})\delta_{\varepsilon_{3l},\varepsilon_{3l'}}-N_3] ,\end{aligned} \tag{5}$$

$$\begin{aligned}\frac{dJ_{12}}{dt}=&\sum_{\varepsilon_{3l}}\frac{-it_R}{\hbar}J_{13}+\sum_{\varepsilon_{1l'}}\frac{-it_L}{\hbar}N_1+\frac{it_L}{\hbar}D_1(\varepsilon_{l1})N_2\\&-\frac{i(\varepsilon_{1l}-\varepsilon_2)}{\hbar}J_{12}-\gamma_{12}J_{12} ,\end{aligned} \tag{6}$$

$$\begin{aligned}\frac{dJ_{23}}{dt}=&\sum_{\varepsilon_{1l}}\frac{it_L}{\hbar}J_{13}+\sum_{\varepsilon_{1l'}}\frac{it_R}{\hbar}N_3-\frac{it_R}{\hbar}D_3(\varepsilon_{3l})N_2\\&+\frac{i(\varepsilon_{3l}-\varepsilon_2)}{\hbar}J_{23}-\gamma_{23}J_{23} ,\end{aligned} \tag{7}$$

$$\begin{aligned}\frac{dJ_{13}}{dt}=&\frac{-it_R}{\hbar}J_{12}D_3(\varepsilon_{3l})+\frac{it_L}{\hbar}J_{23}D_1(\varepsilon_{1l})\\&-\frac{i(\varepsilon_{1l}-\varepsilon_{3l})}{\hbar}J_{13}-\gamma_{13}J_{13} .\end{aligned} \tag{8}$$

Here $D_1(\varepsilon_{1l})$ and $D_3(\varepsilon_{3l})$ are, respectively, the densities of states for the two-dimensional electrons in the electrodes I and III. $F_1(\varepsilon_{1l})$ and $F_3(\varepsilon_{3l})$ are the Fermi distribution functions integrated two dimensionally with respect to k_x and k_y. The variables N_1, N_2, N_3, J_{12}, J_{23}, and J_{13} are similarly defined by the respective two-dimensional integrations of the matrix elements of the density operators $\rho_{1j,1j'}$, $\rho_{2k,2k}$, $\rho_{3m,3m'}$, $\rho_{1j,2k}$, $\rho_{2k,3m}$, and $\rho_{1j,3m}$. Diagonal damping constants γ_{11} and γ_{33} correspond to the longitudinal damping rates at which electrons relax to the thermal equilibrium distribution. The assumption $\gamma_{22}=0$ guarantees conservation of the electron number in the tunneling process. Off-diagonal matrix elements of the density operators include the information about the electron phase. So the off-diagonal damping constants γ_{12}, γ_{23}, and γ_{13} correspond to the phase-smearing rates for electrons.

When the static bias voltage V_0 is applied to the system, the quantum-well energy level for ε_2 as well as the quasi-Fermi-level of the electrons in the right contact decrease, giving rise to the resonant tunneling. When the bias voltage V is changed such that

$$V=V_0+v\exp(i\omega t) , \tag{9}$$

the energy level ε_2 is modulated, which will cause the

modulation of the tunneling current with the angular frequency ω. For simplicity, we assume that ε_2 is modulated as

$$\varepsilon=\varepsilon_2^0-\frac{v}{2}\exp(i\omega t)\ . \tag{10}$$

Here ε_2^0 is the quantum-well energy level under the dc bias voltage V_0.

Here we discuss the case where v is small enough for use to consider only the linear response. The integrated matrix elements are then expressed as

$$\begin{aligned}
N_1&=N_{12}+n_1\exp(i\omega t)\ ,\\
N_2&=N_{2s}+n_2\exp(i\omega t)\ ,\\
N_3&=N_{3s}+n_3\exp(i\omega t)\ ,\\
J_{12}&=J_{12s}+j_{12}\exp(i\omega t)\ ,\\
J_{23}&=J_{23s}+j_{23}\exp(i\omega t)\ ,\\
J_{13}&=J_{13s}+j_{13}\exp(i\omega t)\ .
\end{aligned} \tag{11}$$

Here the variables suffixed with s on the right indicate the mean values of the corresponding integrated matrix elements, and those expressed by small letters are their linear responses to the bias-voltage modulation. It should be noted that these linear-response functions are also functions of electron energy levels, which means that Eq. (11) expresses the infinite number of equations.

Substituting Eqs. (10) and (11) into Eqs. (3)–(8) and taking the terms having $\exp(i\omega t)$, we get the equations for the linear responses. The obtained equations include the information about the mixing of an infinite number of damped quantum oscillators. To solve these equations, we assume that the range of energies of the electrons in the contact is greater than the energies corresponding to the damping constants. It is also assumed that the inelastic tunneling processes gaining or losing modulation quanta[18] can be neglected. The latter assumption may be used when we discuss the case where the modulation frequency is within the order of the damping rates. The summation of the response functions can then be simplified as in the following example:

$$\sum_{\varepsilon_{1l'}}\frac{t_L^2D_1(\varepsilon_{1l'})j_{12}}{\varepsilon_{1l'}-\varepsilon_{1l}+\hbar\omega-i\hbar\gamma_{11}}=i\pi t_L^2D_1(\varepsilon_{1l})j_{12}\ . \tag{12}$$

We thus obtained the following system of equations:

$$[\varepsilon_{1l}-\varepsilon_2^0+\hbar\omega-i\hbar\gamma_{12}-i\pi t_R^2D_3(\varepsilon_{1l})-i\pi t_L^2D_1(\varepsilon_{1l})]j_{12}+i\pi t_L^2D_1(\varepsilon_{1l})j_{21}+i\pi t_Rt_LD_1(\varepsilon_{1l})j_{23}-t_LD_1(\varepsilon_{1l})n_2+\frac{f}{2}J_{12s}=0\ , \tag{13}$$

$$[\varepsilon_2^0-\varepsilon_{3m}+\hbar\omega-i\hbar\gamma_{23}-i\pi t_L^2D_1(\varepsilon_{3m})-i\pi t_R^2D_3(\varepsilon_{3m})]j_{23}+i\pi t_R^2D_3(\varepsilon_{3m})j_{32}+i\pi t_Rt_LD_3(\varepsilon_{3m})j_{12}-t_RD_3(\varepsilon_{3m})n_2-\frac{f}{2}J_{23s}=0\ , \tag{14}$$

$$\sum_{\varepsilon_{1l}}t_L(j_{12}-j_{21})-\sum_{\varepsilon_{3m}}t_R(j_{23}-j_{32})-\hbar\omega n_2=0\ . \tag{15}$$

The procedure to solve this linear equation system is straightforward. n_2 is explicitly solved as

$$n_2=\frac{-\int d\varepsilon\, g'(\varepsilon)[A(\varepsilon)+B(\varepsilon)]}{\int d\varepsilon\, g'(\varepsilon)2[T_Lp'(\varepsilon)-T_Rq'(\varepsilon)]+i\hbar\omega}\frac{f}{2}\ , \tag{16}$$

$$\begin{aligned}
A(\varepsilon)=&-2p'(\varepsilon)t_LJ_{12s}^r+2T_Lr'(\varepsilon)t_RJ_{23s}^r\\
&+\{2p'(\varepsilon)(\varepsilon-\varepsilon_2^0+\hbar\omega)[T_Lt_RJ_{23s}^i-(T_L+\hbar\gamma_{33})t_LJ_{12s}^i]\\
&\quad-2T_Lr'(\varepsilon)(-\varepsilon+\varepsilon_2^0+\hbar\omega)[T_Rt_LJ_{12s}^i-(T_R+\hbar\gamma_{12})t_RJ_{23s}^i]\}/[\hbar\gamma_{12}\hbar\gamma_{23}+\hbar\gamma_{12}T_L+\hbar\gamma_{23}T_R]\ ,
\end{aligned} \tag{17}$$

$$\begin{aligned}
B(\varepsilon)=&2q'(\varepsilon)t_RJ_{23s}^r-2T_Rr'(\varepsilon)t_LJ_{12s}^r\\
&+\{-2q'(\varepsilon)(-\varepsilon+\varepsilon_2^0+\hbar\omega)[T_Rt_LJ_{12s}^i-(T_R+\hbar\gamma_{12})t_RJ_{23s}^i]\\
&\quad+2T_Rr'(\varepsilon)(\varepsilon-\varepsilon_2^0+\hbar\omega)[T_Lt_RJ_{23s}^i-(T_L+\hbar\gamma_{23})t_LJ_{12s}^i]\}/[\hbar\gamma_{12}\hbar\gamma_{23}+\hbar\gamma_{12}T_L+\hbar\gamma_{23}T_R]\ ,
\end{aligned} \tag{18}$$

$$g'(\varepsilon)=\frac{1}{p'(\varepsilon)q'(\varepsilon)-r'(\varepsilon)^2T_LT_R}\ , \tag{19}$$

where

$$p'(\varepsilon)=T_L+2T_R+\hbar\gamma_{23}+\frac{(\hbar\gamma_{12}+T_R)(\varepsilon-\varepsilon_2-\hbar\omega)^2}{\hbar\gamma_{12}\hbar\gamma_{23}+\hbar\gamma_{12}T_L+\hbar\gamma_{23}T_R},$$
$$q'(\varepsilon)=2T_L+T_R+\hbar\gamma_{12}+\frac{(\hbar\gamma_{23}+T_L)(\varepsilon-\varepsilon_2+\hbar\omega)^2}{\hbar\gamma_{12}\hbar\gamma_{23}+\hbar\gamma_{12}T_L+\hbar\gamma_{23}T_R},\tag{20}$$
$$r'(\varepsilon)=1+\frac{(\varepsilon-\varepsilon_2)^2-\hbar\omega^2}{\hbar\gamma_{12}\hbar\gamma_{23}+\hbar\gamma_{12}T_L+\hbar\gamma_{23}T_R}.$$

The normalized coupling constants T_L and T_R are defined by $\pi t_L^2 D_1(\varepsilon)$ and $\pi t_R^2 D_3(\varepsilon)$, respectively, in energy units. J_{12s}^r and J_{23s}^r are the real parts of J_{12s} and J_{23s}, and J_{12s}^i and J_{23s}^i are the imaginary parts. The modulated component of the tunneling current from regions I to II is given by

$$\Delta I_{12}=\frac{ie}{\hbar}\int d\varepsilon\, t_L[j_{12}-j_{21}],\tag{21}$$

which can also be expressed explicitly as

$$\Delta I_{12}=-\frac{e}{\hbar}\left[\frac{f}{2}\int d\varepsilon\, g'(\varepsilon)A(\varepsilon)+n_2\int d\varepsilon\, g'(\varepsilon)2T_L[p'(\varepsilon)-T_R r'(\varepsilon)]/\pi\right].\tag{22}$$

The modulated-current component between regions II and III is defined in the same manner:

$$\Delta I_{23}=-\frac{e}{\hbar}\left[\frac{f}{2}\int d\varepsilon\, g'(\varepsilon)B(\varepsilon)+n_2\int d\varepsilon\, g'(\varepsilon)2T_R[q'(\varepsilon-T_L r'(\varepsilon]/\pi\right].\tag{23}$$

According to Ref. 13, the modulated component of the terminal current ΔI is given by $\Delta I=(\Delta I_{12}+\Delta I_{23})/2$.

In this approach, the tunneling currents from regions I to II and from II to III are described by the imaginary parts of the complex variables j_{12} and j_{23}, which correspond to the dipole moments between the electronic states in the contacts and the quantum well. The frequency responses of the tunneling currents are given by Eqs. (13)–(15), which are nothing but the equations for damped oscillators j_{12} and j_{23} coupled to each other. The energies corresponding to the damping of the oscillators are $\hbar\gamma_{12}+\pi t_R^2 D_3(\varepsilon_{1l})+\pi t_L^2 D_1(\varepsilon_{1l})$ and $\hbar\gamma_{23}+\pi t_R^2 D_3(\varepsilon_{3m})+\pi t_L^2 D_1(\varepsilon_{3m})$. Since the electrons in the contacts with energies around ε_2^0 contribute dominantly to the tunneling process, and the γ_{12} and γ_{23} values are comparable to each other, the damping constant for the resonant-tunneling system is estimated to be

$$\gamma_d=\gamma_{12}+[\pi t_L^2 D_1(\varepsilon_2^0)+\pi t_R^2 D_3(\varepsilon_2^0)]/\hbar.\tag{24}$$

Resonant-tunneling diodes thus respond to external modulation of the voltage up to the frequency of γ_d. There have been many discussions about the tunneling time, which is considered to be a measure of the modulation frequency limit in the double-barrier tunneling devices. Most of them show that the tunneling time depends only on the structure of the scatterers. The present result, however, indicates that the tunneling rate is determined not only by the structure-dependent term $[\pi t_L^2 D_1(\varepsilon_2)+\pi t_R^2 D_3(\varepsilon_2)]/\hbar$ but also by the damping constant γ_{12}, which is the phase-smearing rate caused by the perturbation from the contact electrons. Such a difference comes from the assumption in the present approach that the contact regions are so near to the barrier region that the electron wave in one contact is coherently connected to the wave in the other contact. The motion of the electron wave is thus affected by the perturbation from the reservoir electrons in the contacts.

III. RESONANCE ENHANCEMENT OF THE FREQUENCY RESPONSE

We now give some examples of the tunneling current calculated for the $Al_xGa_{1-x}As$/GaAs double-barrier structure, which can be compared with the reported experimental results.[3] In the calculations, the rectangular potential profile shown by the broken lines in Fig. 1 is used, for simplicity, as a potential under the high electric field. The barrier height is assumed to be 230 meV. Both the quantum-well width w and the barrier width d are 5 nm. The electron density n in each contact is assumed to be 1×10^{18} cm^{-3}, and the ambient temperature is 25 K.

Uncertain parameters in the present formula are the damping constants caused by the perturbation from high-density electrons in the contacts. These parameters may be estimated in a manner similar to that used in Ref. 19, that is, by using the electron-electron interaction Hamiltonian with a screened Coulomb potential. Second-order perturbation theory gives damping-constant values around 10^{13} s^{-1} at room temperature when the electron density is 10^{18} cm^{-3}. The damping constants will be smaller when the ambient temperature is reduced.[20] The interaction between electrons and polar optical phonons in the GaAs material makes a minor contribution to the total damping rates for tunneling electrons. In the actual calculation below, we assume for convenience that $\gamma_{11}=\gamma_{33}=\gamma_{13}=\gamma$ and $\gamma_{12}=\gamma_{23}=\gamma/2$ and use a value around 1×10^{13} s^{-1} for γ. Figure 2 shows the dc characteristics of the tunneling current, when the damping constant γ is varied as a parameter. Clear resonance curves are obtained for the structure with $\gamma<1\times10^{13}$ s^{-1}, while the resonance becomes broader when the value of γ is larger.

Figure 3 shows the frequency response function of the tunneling current to the bias voltage modulation, which is calculated by using Eqs. (22) and (23) for different bias-voltage values. The device structure and the conditions are the same as those used for calculating the curves shown in Fig. 2. γ is fixed to 1×10^{13} s^{-1}. According to this figure, a device with this structure responds to external modulation up to several tens of THz due to the

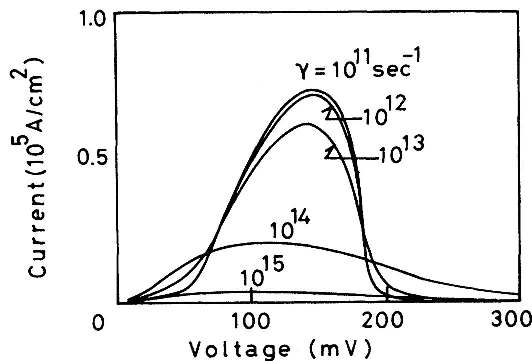

FIG. 2. The dc characteristics of the tunneling current through the GaAs/Al_xGa_{1-x}As double-barrier structure calculated for different damping constants. The electron density n in each contact is 1×10^{18} cm^{-3}, the ambient temperature is 25 K, and the quantum-well width w and the barrier width d are fixed to 5 nm.

enhancements of the response function in the THz region. The γ values at 25 K in the real system may be smaller than the presently assumed values by about an order of magnitude.[20] Even in such a case, we may expect the current response up to the modulation frequency of several THz. The damping constant γ_d of the system is defined by Eq. (24). The γ_{12} value used in the calculation is 0.5×10^{13} s^{-1}. The structure-dependent term $[\pi t_L^2 D_1(\varepsilon_2^0)+\pi t_R^2 D_3(\varepsilon_2^0)]/\hbar$ is calculated to be less than 1×10^{12} s^{-1}, although it depends on the bias voltage. γ_d is thus estimated to be several THz. In a device with the present specific parameters, since the main contribution to γ_d is from the γ_{12} term, the frequency response of the device is more strongly dependent on the phase-smearing rate than on the barrier structure.

The most prominent feature seen in Fig. 3 is the strong enhancement of the response function at a modulation frequency of several THz. In the enhanced region, the response function shows two peaks, as seen in the curve where $F=150$ mV, or one peak and one bottom as in the $F=140$ mV curve. Similar results were obtained for the structures having different parameters. These results suggest that there exist two types of resonances, one around several THz and the other slightly less than 1 THz, and that the phases of the resonances are the same or opposite depending on the bias voltage. The origin of the enhancements is discussed in the following.

The phase shift between the modulated current signal and the voltage modulation signal is calculated as shown in Fig. 4, for the same structure as in Fig. 3. The intense change of the phase shift is seen at a frequency region around THz where the enhancement of the current response is obtained. This implies that the enhancements are originated from some resonance oscillations of the tunneling electrons.

In order to identify the oscillating electrons, we separately calculated the current components ΔI_{12} and ΔI_{23} through the left and right barriers and the number of modulated electrons n_2 in the quantum well, as shown in Fig. 5 for the response function corresponding to $F=150$ mV in Fig. 3. The components ΔI_{12} and ΔI_{23} coincide with each other at low frequencies, but they differ at frequencies near the resonance enhancement of the response function. When the modulation frequency is several THz, for example, only the current component ΔI_{12} oscillates strongly while the other does not. Each resonance frequency thus corresponds to the resonance state of the current component oscillating almost independently through each barrier. Since the peaks in Fig. 3 correspond to these resonance peaks of ΔI_{12} and ΔI_{23} in Fig. 5, the enhancements can be attributed to these resonance oscillations of tunneling electronic through the barriers. Although ΔI_{12} and ΔI_{23} are not the same in this region, the total number of electrons in the ballistic region is conserved, because the electron number n_2 in the quantum well compensates for the difference between ΔI_{12} and ΔI_{23}; that is, the equation $\Delta I_{12}-\Delta I_{23}=n_2$ holds. When the bias voltage is larger than around 150 mV, or in the negative resistance region, as in Fig. 5, ΔI_{12} indicates the same phase as ΔI_{23}. Therefore, the n_2 curve in Fig. 5 shows two peaks, and it becomes zero when

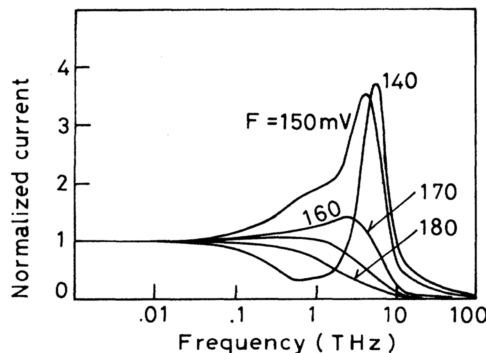

FIG. 3. The frequency response of the tunneling current through the GaAs/Al_xGa_{1-x}As double-barrier structure to the bias-voltage modulation. The mean bias voltage F is varied as a parameter, while the damping constant γ is fixed to 1×10^{13} s^{-1}. Other parameters are the same as in Fig. 2.

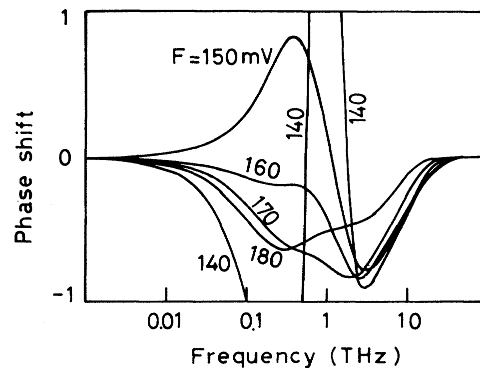

FIG. 4. The phase shift between the modulated current signal and the voltage modulation signal calculated for the double-barrier resonant-tunneling diode having the same structure as in Fig. 3.

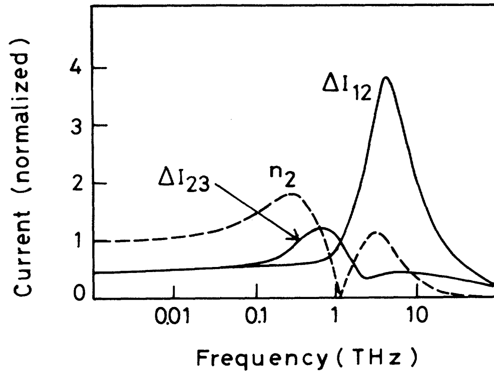

FIG. 5. Frequency response functions of the tunneling currents through the left barrier ΔI_{12} and the right barrier ΔI_{23}, which are compared with that of the number of the electrons in the quantum well n_2. The bias voltage is fixed to 150 mV. Other parameters are the same as those in Fig. 3.

$\Delta I_{12} = \Delta I_{23}$. The corresponding curve for $\Delta I = (\Delta I_{12} + \Delta I_{23})/2$ in Fig. 3 also shows two peaks due to the constructive contributions from ΔI_{12} and ΔI_{23}. On the contrary, the phase of the modulated-current component ΔI_{12} in the positive resistance region, as with the curve for $F = 140$ mV, is opposite to that in the negative resistance region. Thus ΔI_{12} and ΔI_{23} contribute destructively to ΔI. Therefore, the response function for $F = 140$ mV in Fig. 3 indicates a peak and a bottom.

Equations (13)–(15) show that j_{12} and j_{23} are damped oscillators coupled to each other. Since ΔI_{12} or ΔI_{23} is a linear combination of the oscillators j_{12} or j_{23} having different energies, they too are basically damped oscillators. The electron motion is determined on one hand by the coupling between the oscillators that give rise to the electron flow from contacts I to II. On the other hand, each oscillator has its own resonance frequency, which causes the resonance enhancement of the frequency response. This enhancement is well understood by assuming that the coupling between the oscillators is small—that is, that the normalized electron-transfer rates through barriers $\pi t_L^2 D_1(\varepsilon_{1l})/\hbar$, etc. are less than the damping constants γ_{12} and γ_{23}. Equations (13) and (14) then give the formula for the independent motions of j_{12} and j_{23} as

$$j_{12} = \frac{-(f/2)J_{12s}}{\varepsilon_{1l} - \varepsilon_2^0 + \hbar\omega - i\hbar\gamma_{12} - i\pi t_R^2 D_3(\varepsilon_{1l}) - i\pi t_L^2 D_1(\varepsilon_{1l})}, \tag{25}$$

$$j_{23} = \frac{(f/2)J_{23s}}{\varepsilon_2^0 - \varepsilon_{3m} + \hbar\omega - i\hbar\gamma_{23} - i\pi t_L^2 D_1(\varepsilon_{3m}) - i\pi t_R^2 D_3(\varepsilon_{3m})}. \tag{26}$$

Here j_{12} and j_{23} are Lorentzian functions that correspond to Rabi oscillations between the quantum levels of electrons in contacts and the quantum well. Integrating the imaginary parts of j_{12} and j_{23} with respect to the electron energy gives us the modulated components of the total currents ΔI_{12} and ΔI_{23}. If we note that J_{12s} and J_{23s} are energy-dependent Lorentzian-like functions[14] with resonance energy ε_2^0, it is easy to see that the independent motion of the total currents ΔI_{12} and ΔI_{23} exhibit resonance characteristics as a function of the modulation frequency ω. This resonance thus corresponds to the quantum oscillation of the electrons between the quantum-well and contact regions. The resonance frequency is determined by the width of oscillators j_{12} and j_{23}, which can be estimated by using the damping constant γ_d defined by Eq. (24). Therefore, at the high-frequency region around the cutoff frequency, the resonance enhancement is seen as in Fig. 5. The difference between the resonance frequencies of ΔI_{12} and ΔI_{23} is attributed to the deviation of the J_{12s} and J_{23s} functions from the Lorentzian functions.

Figure 6 shows the calculated frequency response of the $Al_xGa_{1-x}As/GaAs$ resonant-tunneling diode with the fixed bias-voltage value of 150 mV for different barrier widths. Other parameters are the same as those used in Fig. 3. The calculated resonance frequency does not depend strongly on the barrier width d. The bandwidth of the frequency response increases slightly when the d value is reduced to smaller than 3 nm. This result can be understood by referring to Eq. (24), which shows that the damping constant for the whole system is the summation of the phase smearing rate γ_{12} and the structure-dependent term. In the present parameter region, the γ_{12} value is dominant in determining γ_d, resulting in the smaller dependence on the barrier structure. The response function for the same parameters with the fixed barrier width of 5 nm is calculated, as shown in Fig. 7, for different damping-constant values. The bias voltage is 150 mV. It turns out that the resonant enhancement is always seen even if the damping constant is changed, although the quantitative values of the frequency bandwidth and the resonance frequency depend on the value of the damping constant. These features are consistent with the above discussion in that the phase-smearing rate

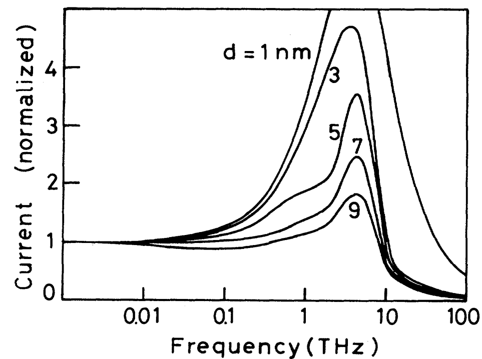

FIG. 6. The frequency response of the $Al_xGa_{1-x}As/GaAs$ resonant-tunneling current with the fixed bias-voltage value of 150 mV for different barrier widths. Other parameters are the same as those used in Fig. 3.

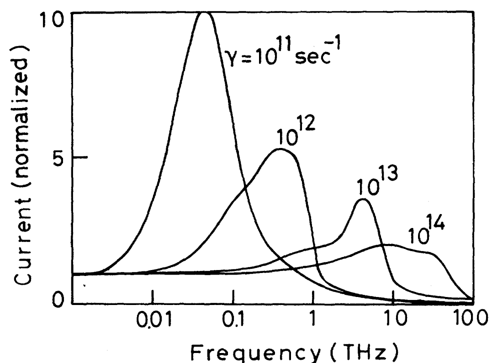

FIG. 7. The frequency response of the $Al_xGa_{1-x}As$/GaAs resonant-tunneling current with the fixed barrier width of 5 nm for different damping constants γ. The bias voltage is 150 mV.

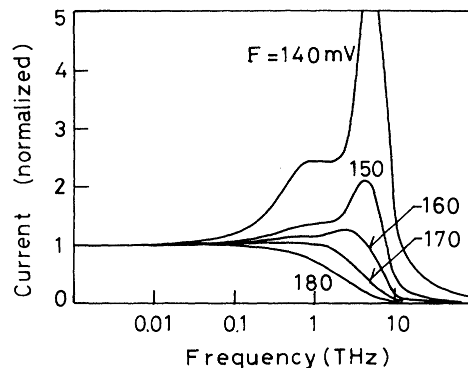

FIG. 9. The room-temperature frequency response of the tunneling current through the $GaAs/Al_xGa_{1-x}As$ double-barrier structure to the small-signal voltage modulation. The damping constant value of 1×10^{13} s^{-1} was used. Other parameters are the same as those in Fig. 2.

γ_{12} plays a crucial role in determining the frequency response of the resonant-tunneling devices.

The enhancement of the current response differs with bias voltage. The calculated bias-voltage dependence of the high-frequency response is shown in Fig. 8 for a modulation frequency of 2.5 THz, which is compared with the dc result. In the region around 145 mV, the dc response is very small, while the high-frequency response is larger. This is derived from the existence of the resonance enhancement of the response function. The position of the minimum and maximum differ between the 2.5-THz curve and the dc curve, and this difference is due to the bias-voltage-dependent resonance enhancement. The bias-voltage dependence of the response is experimentally obtained in Ref. 3. Those experimental data are much more complicated than the curves calculated here but qualitatively consistent with the present calculations.

Numerical examples shown in Figs. 2–8 are calculated only for the ambient temperature of 25 K, in order to compare the results with the reported experiments. The response function for the room-temperature case with the γ value of 1×10^{13} s^{-1} is calculated as shown in Fig. 9.

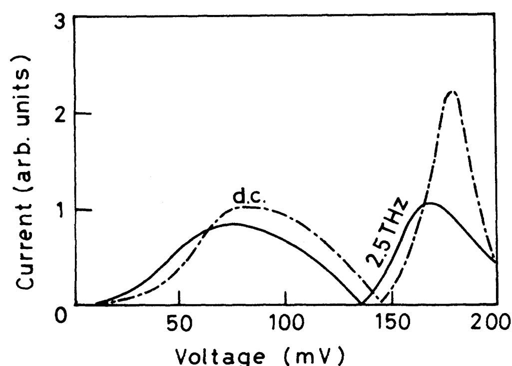

FIG. 8. The bias-voltage dependence of the modulated tunneling current in response to the small-signal voltage modulation of 2.5 THz (solid line) compared with the dc result (broken line). Device parameters are the same as those in Fig. 3.

This result also shows resonance enhancements. In the present treatment, temperature is explicitly included in the equilibrium distribution function for the contact electrons, which dominantly affects static current-voltage characteristics. Dynamic properties are determined primarily by the phase-smearing rates for the tunneling electrons in the contacts. The room-temperature result in this figure is thus similar to the previous figures, because we assumed the same value for γ_{12} in the calculation. However, the γ_{12} value is implicitly dependent on the temperature. If we take into account this effect, the response function shows such temperature dependence that the resonance frequency increases as the temperature increases.

IV. CONCLUSION

The frequency response of the double-barrier resonant-tunneling current was studied theoretically taking into account the effect of the dynamic motion of the contact electrons. The density-matrix approach with a transfer Hamiltonian was used and the effect of the incoherent scatterings in the contacts was modeled with damping constants. We used the boundary condition which does not reject the effects of wave nature in the contacts. Using this approach, the formula for the small-signal frequency response of the device was expressed explicitly. It was shown that the frequency response is determined not only by the structure of the barriers but also by the damping constant γ_{12}, which is the phase-smearing rate for tunneling electrons caused by the perturbation from the contact electrons. The frequency response of the tunneling current exhibits resonance enhancements in the high-frequency region. These are attributed to the quantum oscillations of the electrons between the quantum-well and contact regions.

ACKNOWLEDGMENT

The author is indebted to Dr. Kenju Otsuka for stimulating discussions.

*Present address: Research Center for Advanced Science and Technology, University of Tokyo, Meguro-ku, Tokyo 153, Japan.

[1]R. Tsu and L. Esaki, Appl. Phys. Lett. **22**, 562 (1973).
[2]L. Esaki and L. Chang, Phys. Rev. Lett. **33**, 495 (1974).
[3]T. Sollner, W. Goodhue, P. Tannenwald, C. Parker, and D. Peck, Appl. Phys. Lett. **43**, 588 (1983).
[4]V. J. Goldman, D. C. Tsui, and J. E. Cunningham, Phys. Rev. B **36**, 7635 (1987).
[5]N. S. Wingreen, K. W. Jacobsen, and J. W. Wilkins, Phys. Rev. Lett. **61**, 1396 (1988).
[6]W. Cai, T. F. Zheng, P. Hu, B. Yudanin, and M. Lax, Phys. Rev. Lett. **63**, 418 (1989).
[7]V. J. Goldman, D. C. Tsui, and J. E. Cunningham, Phys. Rev. Lett. **58**, 1256 (1987).
[8]Y. P. Li, A. Zaslavsky, D. C. Tsui, M. Santos, and M. Shayegan, Phys. Rev. B **41**, 8388 (1990).
[9]W. Frensley, Phys. Rev. Lett. **57**, 2853 (1986).
[10]W. Frensley, Phys. Rev. B **36**, 1570 (1987).
[11]W. Frensley, Appl. Phys. Lett. **51**, 448 (1987).
[12]L. Y. Chen and C. S. Ting, Phys. Rev. Lett. **64**, 3159 (1990).
[13]L. Y. Chen and C. S. Ting, Phys. Rev. B **43**, 2097 (1991).
[14]A. Sugimura, Phys. Rev. B **43**, 4276 (1991).
[15]R. K. Lake (unpublished).
[16]M. Lax, Phys. Rev. **145**, 110 (1966).
[17]See, for example, M. Sargent III, M. O. Scully, and W. E. Lamb, Jr., *Laser Physics* (Addison-Wesley, Reading, MA, 1974).
[18]M. Buettiker and R. Landauer, Phys. Rev. Lett. **49**, 1739 (1982).
[19]A. Sugimura, E. Patzak, and P. Meissner, J. Phys. D **19**, 7 (1986).
[20]G. Fasol and H. Sakaki, Solid State Commun. **84**, 77 (1992).